Persistent currents in carbon nanotube based rings

Sylvain Latil*
Groupe de Dynamique des phases condensées, CNRS-Université Montpellier II, France

Stephan Roche
Commissariat à l'Energie Atomique, DSM/DRFMC/SPSMS, 17 avenue des Martyrs, 38054 Grenoble, France

Angel Rubio
Departamento de Física de Materiales, Facultad de Ciencias Químicas, UPV/EHU, Centro Mixto CSIC-UPV/EHU and Donostia International Physics Center (DIPC), San Sebastián/Donostia, Spain

(Received 25 October 2002; revised manuscript received 3 February 2003; published 28 April 2003)

Persistent currents in rings constructed from carbon nanotubes are investigated theoretically. After studying the contribution of finite temperature or quenched disorder on covalent rings, the complexity due to the bundle packing is addressed. The case of interacting nanotori and self-interacting coiled nanotubes are analyzed in detail in relation to experiments.

DOI: 10.1103/PhysRevB.67.165420 PACS number(s): 73.23.Ra, 73.22.−f

I. INTRODUCTION AND BACKGROUND

Carbon nanotubes are micrometer-long hollow cylinders with nanometer scale radii, and electronic properties strongly depending on their geometrical helicity.[1] As promising tools for building up nanoscale electronic devices,[2,3] nanotubes also allow one to challenge the well established common theories of mesoscopic physics. Recently, many works of quantum transport in these systems have revealed puzzling properties resulting from the mixing between their nanometer and micrometer combined length scales.[4–8]

Nanotubes are very particular in the sense that they lie in between small molecular systems such as benzene-type ring molecules, and mesoscopic systems such as metallic or semiconducting wires. In the former entities, basic electronic conduction properties are entirely monitored by the highest occupied–lowest unoccupied molecular orbital (HOMO-LUMO) gap and discrete features of the spectrum, whereas quantum wires may manifest, apart from ballistic transport, band conduction, allowing quantum interference phenomena whenever the full coherence of the wave function is maintained over a reasonable scale.

In metallic single wall nanotubes, at the charge neutrality point there exists some evidence of a Luttinger liquid behavior, namely, that electron-electron interactions are strong enough to deviate the electronic status from Fermi liquid.[9] Besides, a recent work shows that the tube-tube interaction between different nanotube layers is able to induce a transition from the Luttinger liquid to a strongly correlated Fermi system or a Fermi liquid.[10] However, other results on scanning tunneling spectroscopy[11] are fully interpreted in terms of the independent electrons model indicating the importance of screening effects.

Rings of single-walled carbon nanotubes have been synthesized experimentally.[12,13] Depending on the circumference length of the ring, a transition from *n*-type semiconducting to metallic behavior was observed experimentally (from ~ 60 to ~ 1 mm),[14] and further discussed theoretically[15]. Magnetotransport experiments on rings have also been performed,[16] manifesting negative magnetoresistance and weak electron-electron interactions in the low temperature regime. However, no clear Aharonov-Bohm effect was found, in opposition with the properties of the multiwalled nanotube (MWNT) case.[17,18]

An applied magnetic flux Φ is known to induce ring currents in molecules,[19] and persistent currents (PCs) in mesoscopic rings.[20] In fact, every thermodynamic functions of the system are Φ_0-periodic functions of the flux, where $\Phi_0 = h/e$ is the flux quantum. An investigation of PCs then yields valuable information to understand both quantum coherence and dephasing rates.[21,22] These nondissipative currents are intimately related to the nature of eigenfunctions of isolated rings and their flux sensitivity.[20] The manifestation of Φ_0 periodic oscillations of the magnetoresistance or persistent currents is a generic feature that depends on the degree of disorder and the employed averaging procedure.[20,21] Let us introduce a dimensionless flux $\phi = \Phi/\Phi_0$. For noninteracting electrons, the total current at zero temperature is calculated by the following expression:

$$I_{\mathrm{pc}} = -\sum_n \frac{\partial \epsilon_n}{\partial \Phi} = -\frac{1}{\Phi_0}\sum_n \frac{\partial \epsilon_n}{\partial \phi}, \tag{1}$$

with the summation running up to the last occupied energy levels. At a finite temperature T, all the states participate formally to the total free energy, and

$$I_{\mathrm{pc}}(T) = -\frac{1}{\Phi_0}\sum_n \frac{\partial f_n}{\partial \phi}, \tag{2}$$

with

$$f_n = -k_B T \ln\left[1 + \exp\left(\frac{\epsilon_F - \epsilon_n}{k_B T}\right)\right], \tag{3}$$

where ϵ_F is the Fermi level and k_B the Boltzmann constant. In ballistic mesoscopic rings, a perfect agreement between theory and experiments has been reported,[23] differently to diffusive systems (i.e., the mean free path l_e becomes smaller

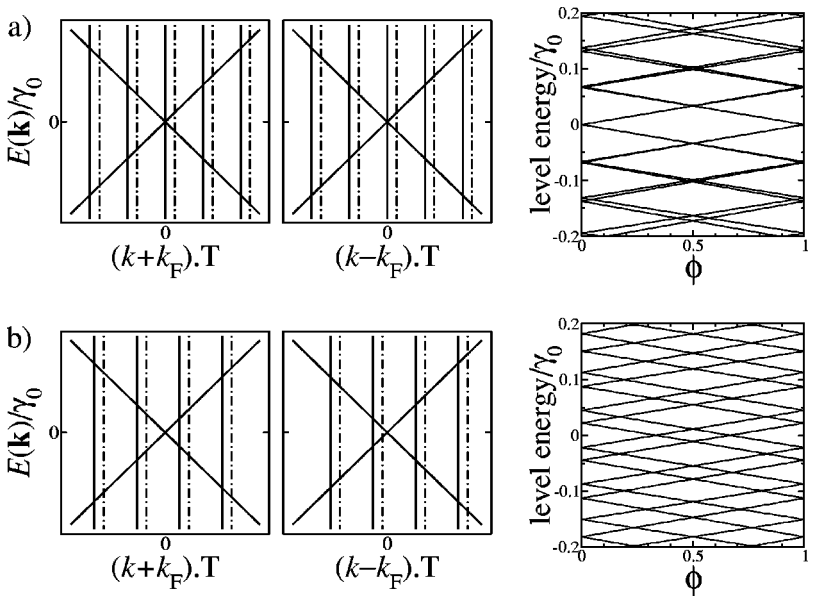

FIG. 1. The cyclic boundary conditions in the nanotorus produces a confinement, responsible of the sampling of the first Brillouin zone of the SWNT. At left a zoom of the vicinity of the crossing points is drawn, the vertical solid lines represent the sampling at zero flux, and the dot-dashed lines the sampling for a nonzero flux. At right, the resulting discrete electronic levels is plotted as a function of the dimensionless flux ϕ. (a) The HOMO-LUMO gap of the type I nanotorus vanishes at zero flux. Application of a magnetic field opens a gap by shifting the sampling of points. (b) The pattern for the type II is more involved since two crossing of levels occurs during the evolution of the flux.

than the ring circumference L_{ring}), for which the discrepancy between the theoretical and the experimental values of PC ($I_{\text{pc}}^{theor.} \sim 10^{-2} I_{\text{pc}}^{expt.}$) remains an open controversy, with electron-electron interactions,[24,25] confinement effects,[26] or nonequilibrium phenomenon[22] as possible explanations. Persistent currents in a Luttinger liquid were analyzed in Ref. 27.

The goal of the present work is to establish to which extent the intrinsic features of carbon nanotubes based ring geometries (helicities of individual tubes, tube-tube interaction, . . .) are reflected on the persistent current patterns in the coherent regime, neglecting electron-electron interactions.

II. PERSISTENT CURRENTS IN A SIMPLE CARBON TORUS

Different works have been published recently on the magnetic properties of simple carbon tori,[28,29] both formally based on a tight-binding (TB) approach. In this paper, the same model is used. It consists in a finite length (n,m) nanotube (containing N primitive cells) curled up onto a torus. Such a torus will be referred to as $(n,m)\times N$. If the circumference L_{ring} of the torus is long enough, the effect of the curvature on the electronic properties is weak and the topologically equivalent system of a straight nanotube with periodic boundary conditions keeps the essential physics. The band structure of this straight tube is calculated with the zone folding technique,[1] keeping only one electron per site and assuming a constant hopping γ_0 between the first neighboring sites. The resulting flux dependent Hamiltonian is

$$H = -\gamma_0 \sum_{i,j(i)} |i\rangle\langle j| \exp(i\varphi_{ij}), \tag{4}$$

$$\varphi_{ij} = 2\pi \left(\frac{z_j - z_i}{L_{\text{ring}}} \right) \phi, \tag{5}$$

where $|i\rangle$ and $|j\rangle$ are the $\pi_\perp$ orbitals located on site, whose positions along tube axis are called z_i and z_j, and $\phi = \Phi/\Phi_0$ is the dimensionless magnetic flux. Since the ring contains N primitive cells, the first Brillouin zone is sampled for a number N of k points, equally separated by $\Delta k = 2\pi/L_{\text{ring}}$, and the linearization of the band structure near the Fermi points implies that the energy level spacing is $\Delta_E = h v_F / L_{\text{ring}}$. In this case, the magnetic flux Φ through the ring acts just as a dephasing rate on the electronic levels, i.e. the sampling of k points in the first Brillouin zone is shifted about $\delta k = \Delta k \phi$.

As reported by Lin and Chuu,[28] there are two kinds of metallic carbon tori. If the Fermi moment is zero, or if the number N of cells is a multiple of 3, then the torus possesses a vanishing HOMO-LUMO gap at zero field (type I). If the Fermi moment is nonzero, and the number of cells is not a multiple of 3, then the torus is sorted onto type II, with a nonvanishing gap at zero field. On the other hand, a semiconducting carbon torus do not exhibit any flux dependent effect.[30]

The physical origin of the persistent currents is the cyclic boundary condition of the electronic system, leading to a sampling of k points in the Brillouin zone. Figure 1 (left) shows this sampling in the vicinity of the Fermi energy, and the resulting discrete spectrum of electronic levels. The application of a magnetic flux dephases the sampling and moves these levels linearly (Zeeman effect) because each k point is related to a magnetic momentum. The linear ϕ dependence of the individual levels is shown in Fig. 1 (right). The resulting persistent current $I_{\text{pc}}(\phi)$, obtain by summing the contribution of each occupied level, is a set of affine functions of the magnetic flux, as shown in Fig. 2. For the type I level with $T=0$, it is

$$I_{\text{pc}}(\phi) = I_0(-1-2\phi), \quad \forall \phi \in [-1/2, 0[, \tag{6}$$

$$I_{\text{pc}}(\phi) = I_0(1-2\phi), \quad \forall \phi \in]0, 1/2], \tag{7}$$

and for the type II level,

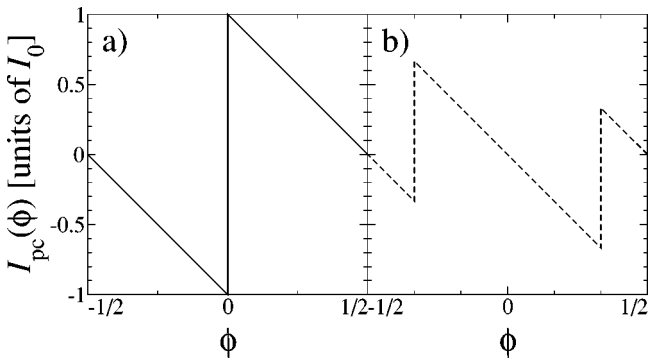

FIG. 2. $I_{pc}(\phi)$ for the two cases I (a) and II (b). The origin of the diamagnetic-paramagnetic transitions are the crossing of levels seen in Fig. 1. I_0 is given by Eq. (11).

$$I_{pc}(\phi)=I_0(-1-2\phi), \quad \forall \phi \in [-1/2,-1/3[, \tag{8}$$

$$I_{pc}(\phi)=-2I_0\phi, \quad \forall \phi \in]-1/3,1/3[, \tag{9}$$

$$I_{pc}(\phi)=I_0(1-2\phi), \quad \forall \phi \in]1/3,1/2], \tag{10}$$

with the value I_0 given by

$$I_0=2N_c e v_F/L_{\text{ring}}, \tag{11}$$

with N_c the number of available channels at Fermi level; $N_c=2$ for metallic nanotubes. Hence, the slope of the function I_{pc} for metallic carbon nanotori is determined by its length only. The reason why the function I_{pc} is not analytical at the points $\phi=0$ and $\phi=\pm 1/3$ is a crossing of eigenenergies at Fermi level (in Fig. 1, right), which provokes a sharp diamagnetic-paramagnetic transition. This work is mainly devoted to the first category of carbon nanotori. Since $I_{pc}(\phi)$ is a periodic and odd function, it can be written down as a Fourier serial like

$$I_{pc}(\phi)=\sum_{n=0}^{\infty} b_n . \sin(2\pi n\phi) \tag{12}$$

with b_n the nth harmonic:

$$b_n=2\int I_{pc}(\phi). \sin(2\pi n\phi)d\phi \tag{13}$$

III. EFFECT OF TEMPERATURE AND DISORDER

In order to investigate the evolution of I_{pc}, with different physical parameters, such as static disorder or electronic temperature, the behavior of two typical currents is analyzed hereafter. The first one is the quadratic flux-averaged current

$$J_{\text{quad}}=\sqrt{\int_{-1/2}^{+1/2} I_{pc}^2(\phi)d\phi}, \tag{14}$$

and the second is the absolute value of I_{pc} for the quarter of the quantum flux, which is related to the intensity of the first harmonic:

$$J_{1/4}=\left|I_{pc}\left(\frac{1}{4}\right)\right|. \tag{15}$$

We first analyze the effect of temperature on the intensity of PCs. Here, we still assume that the phase coherence length L_φ is much larger than L_{ring}, so that the system remains fully described by the eigenfunctions of its Hamiltonian. The electrons are independent and the effect of temperature is to induce a distribution of the occupancy around ϵ_F, within k_BT. $I_{pc}(\phi)$ is given by Eq. (2). As shown in the left part of Fig. 3, the effect of T is a smoothing of the sawtooth shape of the PCs, which became fully analytical functions. This means that the harmonics of higher order are the first to be affected by temperature. On the right side of Fig. 3 is plotted the evolution of the typical currents versus the temperature. The behavior is simple: below a critical temperature T^* the function J_{quad} decreases slightly and $J_{1/4}$ is a constant. Above the transition, both are exponentially damped. The effect of T on the PC of linear chains or one-dimensional (1D) free electrons systems has been investigated by Cheung *et al.*,[31] who demonstrated that for every shape of band structure, a temperature transition can be defined as

$$T^*=\frac{\Delta_E}{2\pi^2}, \tag{16}$$

where $\Delta_E=h.v_F/L_{\text{ring}}$ is the level spacing at Fermi energy. When $T>T^*$ the function $I_{pc}(\phi)$ is fairly approximated by its first harmonic, and since this harmonic is the last to be affected, the typical currents decrease drastically after the transition.

It is worth to noting that the behavior of such tubular system is exactly the same that a linear chain or 1D free

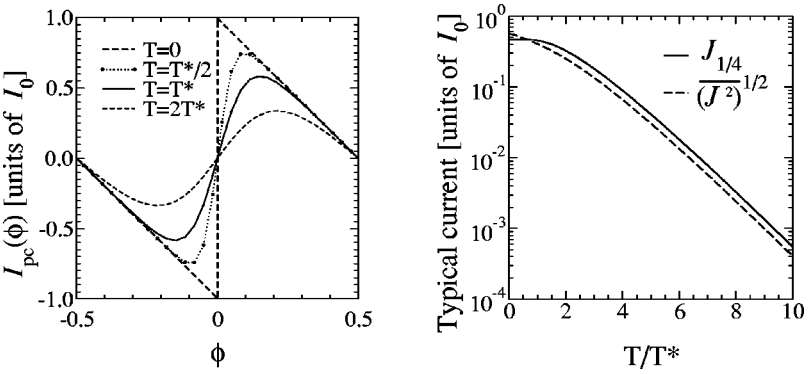

FIG. 3. Left: Temperature effect on the persistent $I_{pc}(\phi)$. Right: Semilog plot of the temperature dependent typical currents. As happens for the linear chain of atoms (Ref. 31), these currents exhibit a transition temperature, namely, T^* (see the text), from which the intensity decreases exponentially.

electrons systems. This effect is due to the small number of channels available in a carbon nanotube ($N_c=2$). In fact, no effect on the radius of the nanotube occurs. In that sense, defect free metallic nanotubes behave like real one-dimensional systems.

We turn now to an analysis of the effect of a quenched disorder on the persistent current, with a particular focus on the typical value of the averaged current, in order to compare the results with established theories. To discuss the effect of a conduction mechanism on persistent currents, static disorder is simulated by a random modulation of the on-site energies.[32] Particular attention is paid to the behavior of PC close to the transition between ballistic and more localized conduction regimes. Since the application of this static disorder breaks the translational symmetry, the whole structure (and no longer a single unit cell) is conserved to solve the eigenproblem. As a generic case of metallic tubes the (6,6) armchair nanotube (radius $R\simeq 2.58$ nm) is considered. The length of the tube is 75 unit cells, implying a perimeter of about $L_{\rm ring}\simeq 18.4$ nm, and a single particle level spacing at Fermi energy $\Delta_E\simeq 0.205$ eV. Randomly fluctuating on-site energies are added to the former ϕ-dependent TB Hamiltonian (4) like

$$H=\sum_i \varepsilon(i)|i\rangle\langle i|-\gamma_0\sum_{i,j(i)}|i\rangle\langle j|\exp(i\varphi_{ij}), \qquad (17)$$

where φ_{ij} is given by Eq. (5), and $\varepsilon(i)$ is the randomly modulated on-site energy of the ith atom. The range of the on-site energy fluctuation is $[-W/2,W/2]$, where W is the disorder strength. This modulation enables to tune an important physical transport length scale in nanotubes, namely the electronic mean free path which given by (for the armchair (n,n) nanotubes[4,5])

$$l_e\simeq 6\sqrt{3}na_{\rm cc}\left(\frac{\gamma_0}{W}\right)^2, \qquad (18)$$

where $a_{\rm cc}=1.42$ Å is the distance between two carbon atoms of the honeycomb lattice. Since this formula derives from the Fermi golden rule, it should be valid in the limit of weak scattering and for Fermi energies close to the charge neutrality point. An important feature, which is not common in mesoscopic wires, is that, in first approximation, the mean free path scales with the diameter.

In mesoscopic systems, the quantity l_e discriminates between three different physical conduction regimes: the ballistic motion for $l_e>L_{\rm ring}$, the diffusive regime $l_e<L_{\rm ring}$, and the localized regime whenever $\xi\simeq N_c l_e<L_{\rm ring}$.[33] A single level of energy ϵ_n carries a current $I_n(\phi)$. In the diffusive regimes of mesoscopic systems, the typical current carried by this single level $J_{\rm typ}^{(n)}$ reads[31,34,35]

$$J_{\rm typ}^{(n)}=\sqrt{\langle\overline{I_n^2(\Phi)}\rangle_{W,L_{\rm ring}}}\sim\frac{\sqrt{\Delta E_c}}{\Phi_0}, \qquad (19)$$

where $\langle\cdots\rangle$ denotes the average value over disorder strength and system length, and $\overline{I_n^2(\Phi)}$ is the flux-average current. The typical total current has been found to be of the order of

$$J_{\rm typ}=\sum_n J_{\rm typ}^{(n)}\sim\frac{E_c}{\Phi_0}=\frac{ev_F l_e}{L_{\rm ring}^2}, \qquad (20)$$

where $E_c=\hbar D/L_{\rm ring}^2=\hbar v_F l_e/L_{\rm ring}^2$ is the Thouless energy (diffusivity constant is D). Differently, the effect of disorder on persistent current remains a complex nonelucidated problem in the ballistic limit.[36]

To extract the effect of disorder on persistent currents, we thus follow their W dependence. A first observation is that both behaviors of $J_{\rm quad}$ and $J_{1/4}$ are reminiscent of the temperature dependent patterns. We plot the W dependence of the two typical currents in Fig. 4(a) for a number of random disorder configurations, and the resulting average. The behavior of $J_{1/4}$ is particularly illustrative since its flux dependence is mainly dominated by the first harmonic. We also plot, in Fig. 4(b), the dependence of $J_{\rm quad}$ and $J_{1/4}$ upon the equivalent mean free path $l_e(W)$, that is given by Eq. (18). Both are exponentially damped as soon as $2l_e<L_{\rm ring}$ which corresponds to $W\geqslant 1.83\times\gamma_0$.

For smaller disorder, behaviors become more difficult to interpret within the framework of conventional theory. For a diffusive regime, one would expect an averaged persistent current following $\sim ev_F l_e/L_{\rm ring}^2$ so reduced by a factor of $\sim l_e/L_{\rm ring}$ with respect to the ballistic case. This would yield a $(\gamma_0/W)^2$ dependence of the amplitude with disorder strength. However, from our results, the damping of $J_{1/4}$ and $J_{\rm quad}$ are much smaller, especially for $l_e<L_{\rm ring}$. It is indeed rather difficult to extract the W dependence in the ballistic regime, since all harmonics respond differently to a given disorder strength. Actually, as long as $nL_{\rm ring}<l_e$, the harmonic of rank n remains nearly unaffected by disorder, whereas harmonics with $nL_{\rm ring}>2l_e$ are exponentially damped. In conclusion, except from strong disorder cases, persistent currents in covalent rings of carbon nanotubes are weakly sensitive to disorder and their amplitude remain close to that of the clean ballistic case.

IV. FROM A SIMPLE TORUS TO A BUNDLE

The systems studied in the preceding sections are useful to understand the physical phenomena in carbon nanotubes, but seem far to be a reliable representation for describing the full complexity of nanotube based rings. The bonding nature of the closing of the ring of single walled nanotubes (SWNTs) has been suggested either to be covalent[12] or of Van der Waals type.[13] In any case, the synthesized rings are constituted by SWNTs closely packed in bundles. They contains from tens to hundreds of individuals nanotubes, whose interaction are likely to control electronic pathways along the ring.

The study of these complex system is difficult due to the large number of involved carbon atoms. First, the bundle packing effect will be scrutinized [drawn in Fig. 5(a)]. Our goal is to understand how relevant is the Van der Waals interaction between rings and how it affects the persistent current patterns. Second, following some experimental observations,[13] imperfect tori made with a curled nanotube [as shown in Fig. 5(b)] will be under consideration. These

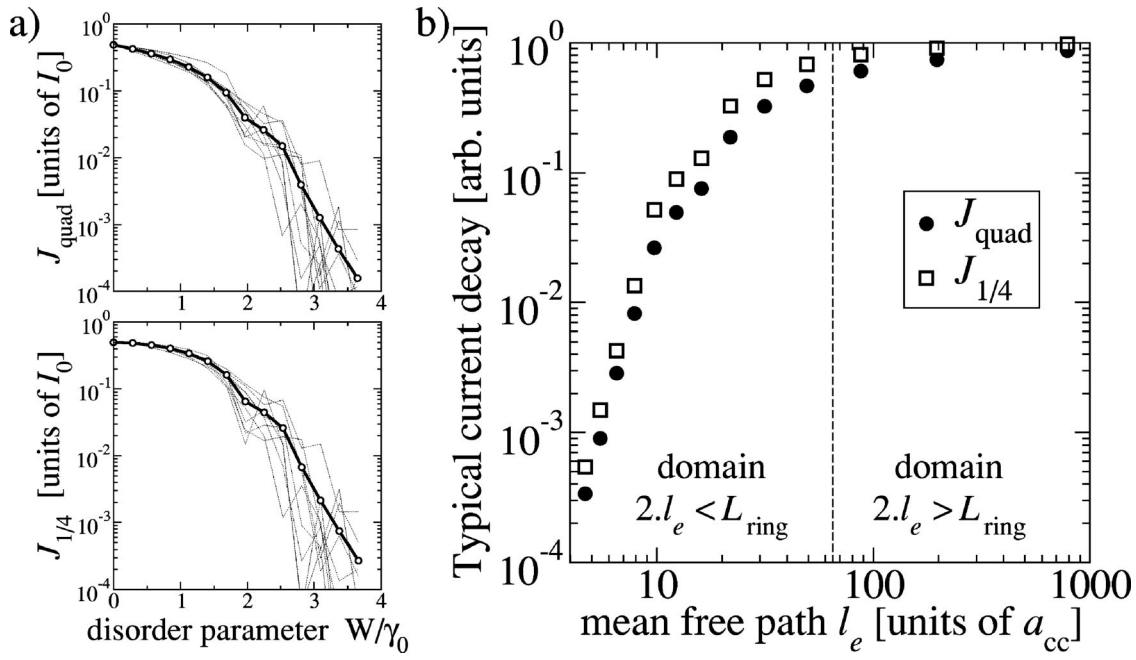

FIG. 4. (a) Semilog plot of the typical currents J_{quad} (up) and $J_{1/4}$ (bottom) vs the disorder strength. The dashed lines describe different disorder configurations, their average is identified by the bold line with circles. (b) Log-log plot of the typical currents as function of mean free path l_e, given by Eq. (18). The transition from a ballistic (small W, long l_e) to a more localized (larger W, short l_e) is pointed out by a vertical line, at which W yields $L_{ring}=2.l_e$.

two models allow one to envision the bundle effect on large ring systems.

The study of persistent currents, when a torus-torus interaction is turned on, is done by constructing a model of a bundle. This consists of sticking two of these objects (namely A and B), and allowing them to interact with an *ad hoc* potential. This tube-tube hopping, that we call γ_1, was optimized to reproduce correctly the electronic properties of 3D graphite[37] or MWNTs.[38] Such a tube-tube interaction between two tori is believed to affect the shape or the intensity of $I_{pc}(\phi)$ in various ways. The Hamiltonian is now

$$H=H_A+H_B-\gamma_1\sum_{\langle i,p\rangle}(|i\rangle\langle p|+|p\rangle\langle i|)\exp(i\varphi_{ij}). \quad (21)$$

H_A and H_B are the Hamiltonians [Eq. (4)] of the noninteracting rings, and $|i\rangle$ (respectively $|p\rangle$) is a $p_\perp$ orbital of the A (respectively B) torus. The phase φ_{ij} is given by Eq. (5), and the secondary hopping integral is

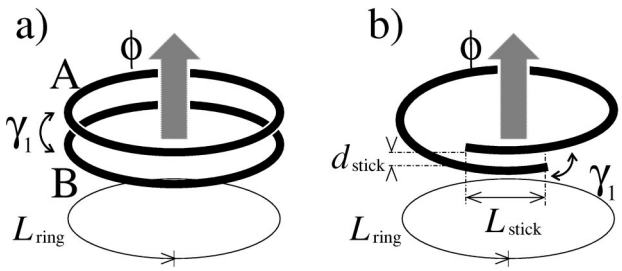

FIG. 5. (a) A complex ring made of two interacting carbon nanotori. (b) A coil shaped carbon nanotube.

$$\gamma_1=V_{int}\exp\left(\frac{d-\delta}{l}\right), \quad (22)$$

where d denotes the relative distance between the two sites. We take the value $\gamma_0=2.9$ eV, which allows the TB model to fit experimental data.[39] The other parameters are $V_{int}=0.36$ eV, $\delta=3.34$ Å, and $l=0.45$ Å. To simplify the comparison with precedent sections, γ_0 is kept as the energy unit.

It is important to note that the two subsystems are forced to have the same circumference, hence the field corresponding to $\Phi=\Phi_0$ is the same in the two cases. If there are multiple correspondences between the magnetic flux and field, and the Φ_0 periodicity is ill defined. As such a situation may happen, we should avoid it to extract the effect of the tube-tube interaction. The choice of the subsystems is then restricted to equivalent helicities [e.g. two armchair tubes, two zigzag tubes, two $(3n,2n)$, etc.]. The distance between the tube walls is fixed to $\simeq 3.4$ Å.

Our calculations show first that a semiconducting tube has no effect on the persistent current of a metallic one. We can imagine the distribution of states of the interacting tori as two quasicontinua under interaction. The resulting quasicontinuum, which is the set containing all the eigenstates of the total system, is a mixing of the eigenstates of each noninteracting subsystem. However the mixing rate is proportional to $\delta(\epsilon_i-\epsilon_j)$, where ϵ_i and ϵ_j are the two considered eigenvalues of each free torus. Hence coupling within the gap of the semiconducting torus happens. Moreover, the persistent current in the metallic torus is carried by the levels around ϵ_F, where the semiconducting tube does not have any state; then the persistent current of the complex system is equal to the persistent current of the free metallic torus.

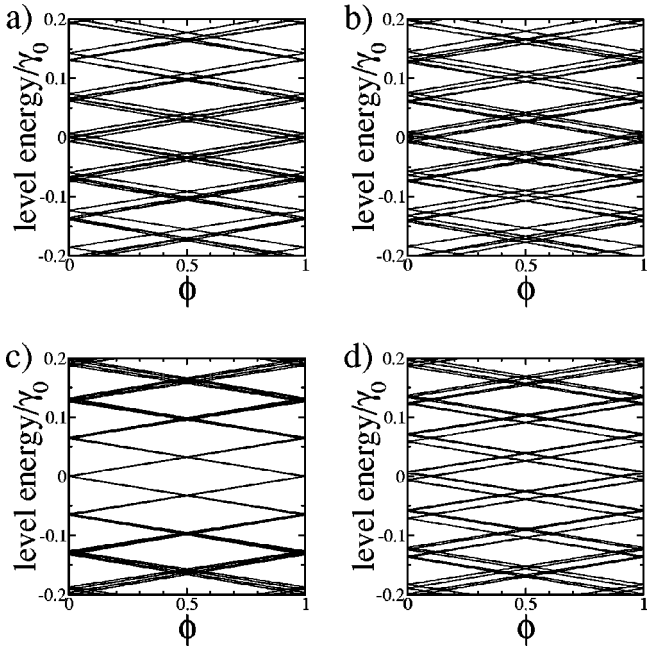

FIG. 6. Discrete levels of two interacting tori, as function of flux. (a) Two $(7,7)\times 84$ tori. The tube-tube interaction induces a lifting of degeneracies. (b) Two $(7,7)\times 84$ tori, with different orientation. (c) A $(7,7)\times 84+(11,2)\times 12$ noncommensurate system. It is fairly similar to the non-interacting case (see Fig. 1). (d) A $(11,2)\times 12+(2,11)\times 12$ commensurate system.

Interesting cases arise whenever two metallic tori are interacting. The studied bundle is made of two (7,7) tori containing 84 primitive cells (they are type I tori, with a degenerated Fermi level). By varying the relative orientations of the two tubes before curling them, and since the interaction γ_1 depends upon the geometry of the two subsystems, different cases of interaction schemes are explored. As shown in Fig. 6(a) and 6(b), the tube-tube interaction induces a HOMO-LUMO gap at zero flux, and breaks level degeneracies. The flux-dependent evolution of the discrete levels shows that several crossings between eigenstates are driven by increasing magnetic flux, until the pattern returns to its original configuration when $\Phi=\Phi_0$. Since the value of the discrete energy levels changes from one orientation to another, the different level crossings induce modifications of the shape of $I_{\mathrm{pc}}(\phi)$. However, the slope of the currents, which depends on the circumference and the Fermi velocity only, is unaffected. In Fig. 7 is shown the function $I_{\mathrm{pc}}(\phi)$ for the two former cases and for the free tori is shown. Hence, in all cases, the tube-tube interaction will reduce the typical persistent current when compared to the isolated torus.

Obviously, the precedent system is far to be a generic case, since the chosen torus is one of the highest symmetry. Moreover, each subsystem is just the mirror image of the other one. The effect of incommensurability is then addressed considering two different metallic SWNTs, with similar diameter [the (7,7) and (11,2) have same radii and the length cell of the latter is exactly seven times the length cell of the former]. After checking that the magnetic properties of the $(7,7)\times 84$ torus are exactly the same as the $(11,2)\times 12$ torus the study of the bundle composed by one

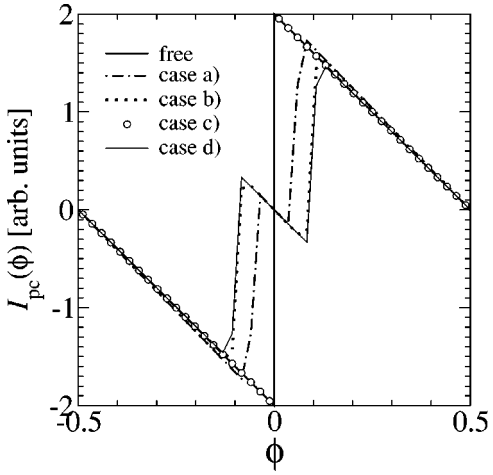

FIG. 7. Flux dependent persistent currents, for the same cases as Fig. 6. The shape $I_{\mathrm{pc}}(\phi)$ for cases (a), (b), and (d) is due to the crossing of levels at Fermi energy. The noncommensurate structure (case c) behaves similarly to the free tori.

(7,7) torus containing 84 periods and one (11,2) torus containing 12 periods is made. In this case even though the ring is by definition L_{ring} periodic ($L_{\mathrm{ring}}=2.07$ nm here), the disorder-free bundle becomes quite different from the previous cases since there is now incommensurability at short scale. The resulting discrete levels are plotted as a function of the flux in Fig. 6(c). Close to the charge neutrality, the evolution of the levels is very similar to those of the single torus. Then, in the incommensurate case, the tube tube interaction is not able to open a HOMO-LUMO gap, and the persistent current (also shown in Fig. 7) is roughly equivalent to twice the one of the free torus.

Consequently, in this case, the tube-tube interaction could act as a static disorder, with a modulation strength $W=\langle\gamma_1\rangle\sim\gamma_0/10$. As discussed in Sec. III, this range of disorder induces no relevant perturbations on the persistent currents, and explains why the PCs of noncommensurate tori are not affected by tube-tube interactions.

Finally, a last check is done. The Fig. 6(d) shows the discrete levels of the $(11,2)+(2,11)$ structure. A splitting of levels is present, and is of the same order of magnitude as that of the $(7,7)+(7,7)$ case. This means that the physical reason of absence of perturbation of PCs is an effect of short range incommensurability and is not intrinsic to the underlying chirality.

V. COILED NANOTUBES

In this part we are concerned with coiled nanotubes. These structures are imperfectly closed nanotori, which are rolled up with finite length nanotubes. The two ends of the nanotube are sticked through a van der Waals interaction, as shown in Fig. 5(b). The circumference of the curled system L_{ring} is necessarily shorter than the length of the uncurled structure; otherwise sticking is impossible. The length of the sticking area is noted as L_{stick}, while the distance between the two tubes' ends is d_{stick}. Of course, these three parameters can vary within a given bundle and, depending on their

relative values, different patterns of $I_{pc}(\phi)$ will result.

If we restrict the working space to the $|p_\perp\rangle$ orbitals, the electronic Hamiltonian takes the following expression:

$$H = H_0 - \gamma_1 \sum_{\langle i,p \rangle} (|i\rangle\langle p| + |p\rangle\langle i|), \tag{23}$$

with H_0 the Hamiltonian of the uncurled structure, and γ_1 defined by Eq. (22). Now the sum runs for the orbitals $|i\rangle$ (respectively $|p\rangle$) located on the right (respectively left) extremity of the nanotube. Since the second part is clearly less important than the first it can be seen as a perturbation. This means that the most relevant part of the Hamiltonian describes an uncurled finite length nanotube. Such kinds of structures have been intensively investigated during the last years.[40–42] They exhibit a ''particle-in-a-box'' behavior which implies an important interplay between the total length $L_{\text{ring}} + L_{\text{stick}}$, chirality, and HOMO-LUMO gap properties: the gap is zero when the Fermi moment is nonzero, and the number of primitive cells within the structure is $3q+1$ (i.e., corresponding to the type I tori), otherwise the gap is nonzero (corresponding to the type II tori). The principal difference from the torus is that the rotational symmetry is lost, and the resulting electronic pathways around the ring are completely driven by the intertube hopping at the edges. The probability of hopping from one extremity to the other one will then depend on the geometry of the eigenstates around ϵ_F, then upon the length and the chirality of the used nanotube.

Calculations were done on the (5,5) nanotube, with open ends. The parameter d_{stick} monitors the interlayer hopping value, since γ_1 depends on the distance [Eq. (22)]. As shown in Fig. 8 (top), the results show that the intensity of $I_{pc}(\phi)$ is weakly dependent on the parameter d_{stick}, whereas the shape is not affected. The dependence on the sticking length L_{stick} is drawn in Fig. 8 (bottom), keeping L_{ring} constant, showing the resonances according to the ''particle-in-a-box'' model. The shape is strongly dependent on the length—or the number of unit cells—of the curled tube: adding one unit cell could switch the response from diamagnetic to paramagnetic, and if the length is resonant (the gap is minimal), the function $I_{pc}(\phi)$ is quasi $\Phi_0/2$-periodic. In all cases, the intensity of PCs is one order of magnitude lower than in the ideal case.

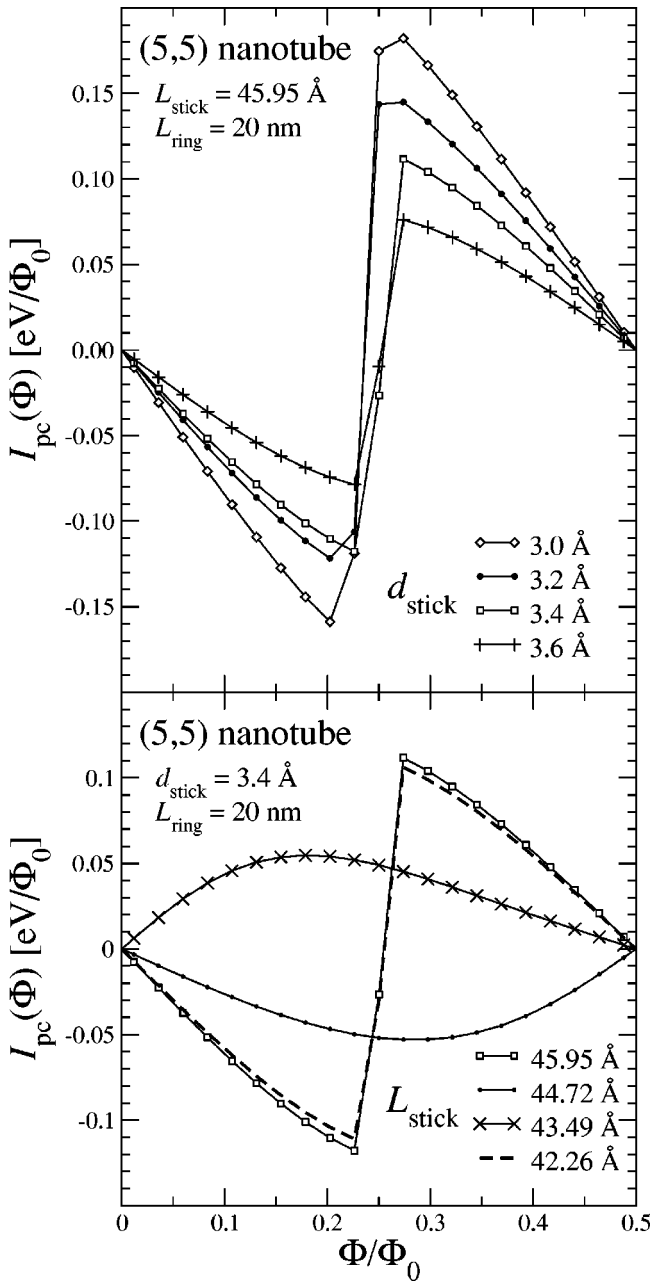

FIG. 8. Flux dependent persistent currents induced in coiled nanotubes. Top: Evolution with respect to d_{stick} for fixed L_{stick} and L_{ring}. Bottom: Illustration of the effect of increasing L_{stick} while keeping L_{ring} and d_{stick} unchanged.

VI. SLATER-KOSTER APPROACH

Until now, our study of the electronic properties of nanotori was limited to $|p_\perp\rangle$ orbitals only. This approach is equivalent to the zone folding technique. We know that this model presents some discrepancies compared to more refined calculations. More precisely, the curvature needed to roll up the sheet onto a tube, and the resulting $\sigma-\pi$ mixing, are responsible for a gap opening in the band structure of all the nonarmchair metallic nanotubes, and for a light shifting of the Fermi moment k_F of armchair nanotubes, that keep a real metallic behavior. Although these modifications are not spectacular, they directly affect the states just around the Fermi level. Since these states are carrying a persistent current, we need to study $I_{pc}(\phi)$ for nanotori described by a more accurate approach than the zone folding technique.

Calculations were done with an orthogonal tight-binding Hamiltonian with a Slater-Koster description of the hopping integrals. The parameters used are those of Louie and Tománek,[43] but trials with Charlier-, Gonze-Michenaud[44] parameters give the same results. The gap of metallic nanotubes is estimated as $\simeq 0.106$ eV, that is very large compared to the level separation for zone folding method $\Delta E = 2\pi v_F/L$. At the scale of this energy ΔE, the ''metallic'' nanotubes behave exactly like insulators: the magnetically

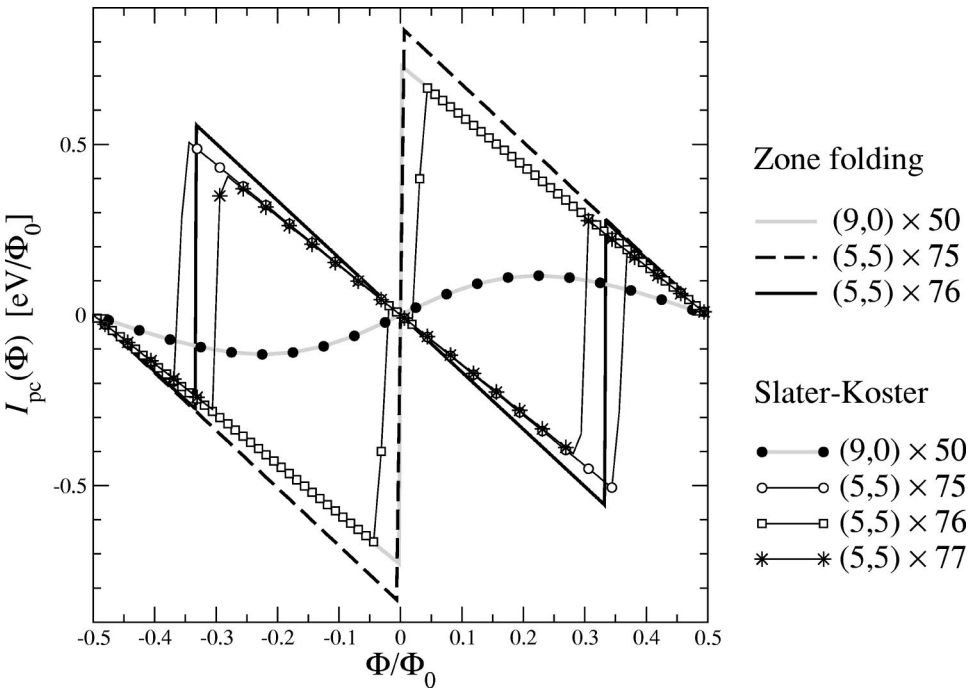

FIG. 9. Comparison of persistent currents obtained for the (9,0) nanotorus with the zone-folding method (thin lines) and the Slater-Koster approach (thick lines).

induced current is small, as shown in Fig. 9 for a (9,0) based nanotorus.

However, the armchair nanotubes preserve band crossings at Fermi level, which means that armchair based nanotori (and only them) will still exhibit persistent currents. However, the Fermi moment k_F is no longer located at two-thirds of the Brillouin zone; hence the concept of type I and II nanotori (with crossing of levels when $\Phi=0$, or not) loses its meaning. All the nanotori possess a nonvanishing HOMO-LUMO gap for zero flux, and the crossing of levels does not happen exactly at the value $\Phi=\pm\frac{2}{3}\Phi_0$. As a consequence, there are more level crossings at charge neutrality point within the $[-\Phi_0/2,\Phi_0/2]$, as shown also on Fig. 9, leading to a stronger weight of the higher harmonics in the Fourier spectrum. Compared to the zone folding results, we can then expect an increased sensitivity of the induced current, with temperature or disorder.

VII. CONCLUSION AND PERSPECTIVES

In this work, a study of persistent current in nanotube based rings has been presented. It was first pointed out that disorder and temperature diminish the persistent currents in nanotori in a similar fashion as they do in 1D systems, assuming a Fermi energy at the charge neutrality point. Further, it has been established that tube-tube interaction does not affect the shape and intensity of $I_{pc}(\Phi)$, except in the rare cases of commensurate systems.

On the other hand, the necessity of intertube hopping to convey electrons along a closed path was shown to weakly damp the magnitude of typical PCs. Moreover, if the curvature induced σ-π mixing is taken onto account in the model, then the persistent currents are completely screened, except for the armchair based nanotori.

This suggests that such a quantity may fluctuate significantly from one bundle to another, and that it should be strongly reduced in regards to the specific pattern found in pure tori.[45] If, for some reasons (doping, etc . . .) the Fermi level is sufficiently shifted away from the charge neutrality point, then a linear dispersion relation is predicted for nonarmchair metallic tubes. Hence in this case, the persistent current may be as strong as the one of armchair based nanotori.

ACKNOWLEDGMENTS

This work was supported by European Community through the COMELCAN network (HPRN-CT-2000-00128). Professor R. Saito and Professor J. C. Charlier are acknowledged for valuable discussions.

*Present address: Unité PCPM, Université Catholique de Louvain, Bâtiment Boltzmann, Place Croix du Sud 1, B-1348 Louvain-la-Neuve, Belgium.

[1] R. Saito, G. Dresselhaus, and M. S. Dresselhaus, *Physical Properties of Carbon Nanotubes* (Imperial College Press, London, 1998).

[2] S. Tans, A. Verschueren, and C. Dekker, Nature (London) **393**, 49 (1998); A. Bachtold, P. Hadley, T. Nakanishi, and C. Dekker, Science **294**, 1317 (2001).

[3] R. Martel, T. Schmidt, H. R. Shea, T. Hertel, and Ph. Avouris, Appl. Phys. Lett. **73**, 2447 (1998); F. Leonard and J. Tersoff, Phys. Rev. Lett. **88**, 258302 (2002); S. Heinze, J. Tersoff, R. Martel, V. Derycke, J. Appenzeller, and Ph. Avouris, *ibid.* **89**, 106801 (2002); J. Appenzeller, J. Knoch, V. Derycke, R. Martel, S. Wind, and Ph. Avouris, *ibid.* **89**, 126801 (2002).

[4] C. White and T. Todorov, Nature (London) **393**, 240 (1998); T.

Ando, Semicond. Sci. Technol. **15**, R13 (2000).
[5] S. Roche, G. Dresselhaus, M. Dresselhaus, and R. Saito, Phys. Rev. B **62**, 16092 (2000); S. Roche and R. Saito, Phys. Rev. Lett. **87**, 246803 (2001).
[6] P. Poncharal, C. Berger, Y. Yi, Z. L. Wang, and Walt A. de Heer, J. Phys. Chem. **106**, 12104 (2002).
[7] S. Roche, F. Triozon, A. Rubio, and D. Mayou, Phys. Lett. A **285**, 94 (2001); Phys. Rev. B **64**, 121401 (2001).
[8] H. Suzuura and T. Ando, Mol. Cryst. Liq. Cryst. **340**, 731 (2000).
[9] M. Bockrath, D. H. Cobden, J. Lu, A. G. Rinzler, R. E. Smalley, L. Balents, and P. L. McEuen, Nature (London) **397**, 598 (1999).
[10] R. Egger, Phys. Rev. Lett. **83**, 5547 (1999); E. Arrigoni, Phys. Rev. B **61**, 7909 (2001); R. Egger and A. Gogolin, Phys. Rev. Lett. **87**, 066401 (2001).
[11] T. W. Odom, J.-L. Huang, P. Kim, and C. M. Lieber, J. Phys. Chem. B **104**, 2794 (2000).
[12] J. Liu, H. Dai, J. H. Hafner, D. T. Colbert, R. E. Smalley, S. J. Tans, and C. Dekker, Nature (London) **385**, 780 (1997).
[13] R. Martel, H. R. Shea, and P. Avouris, Nature (London) **398**, 299 (1999); J. Phys. Chem. B **103**, 7551 (1999).
[14] H. Watanabe, C. Manabe, T. Shigematsu, and M. Shimizu, Appl. Phys. Lett. **78**, 2928 (2001).
[15] G. Cubernati, J. Yi, and M. Porto, Appl. Phys. Lett. **81**, 850 (2002).
[16] H. Shea, R. Martel, and P. Avouris, Phys. Rev. Lett. **84**, 4441 (2000).
[17] C. Schönenberger, A. Bachtold, C. Strunk, J.-P. Salvetat, and L. Forr, Appl. Phys. A: Mater. Sci. Process. **69**, 283 (1999).
[18] A. Fujiwara, K. Tomiyama, H. Suematsu, M. Yumura, and K. Uchida, Phys. Rev. B **60**, 13492 (1999).
[19] F. London, J. Phys. Radium **8**, 397 (1937).
[20] M. Buttiker, Y. Imry, and R. Landauer, Phys. Lett. A **96**, 365 (1983); L. P. Lévy, G. Dolan, J. Dunsmuir, and H. Bouchiat, Phys. Rev. Lett. **64**, 2074 (1990).
[21] N. Trivedi and D. A. Browne, Phys. Rev. B **38**, 9581 (1988).
[22] V. E. Kravtsov and B. L. Altshuler, Phys. Rev. Lett. **84**, 3394 (2000).
[23] D. Mailly, C. Chapelier, and A. Benoit, Phys. Rev. Lett. **70**, 2020 (1993).
[24] V. Ambegaokar and U. Eckern, Phys. Rev. Lett. **65**, 381 (1990).
[25] T. Giamarchi and B. S. Shastry, Phys. Rev. B **51**, 10915 (1995).
[26] V. M. Appel, G. Chiappe, and M. J. Sánchez, Phys. Rev. Lett. **85**, 4152 (2000).
[27] D. Loss, Phys. Rev. Lett. **69**, 343 (1992).
[28] M. F. Lin and D. S. Chuu, Phys. Rev. B **57**, 6731 (1998).
[29] M. Margánska and M. Szopa, Acta Phys. Pol. **B32**, 427 (2001).
[30] In fact, there is a little modification of the energy, due to a magnetization M induced by the magnetic flux Φ as $M \sim \chi_m . \Phi$, where χ_m is the magnetic susceptibility, equivalent to susceptibility of straight nanotube. However, since this magnetization does not exhibit any Φ/Φ_0 behavior, we ignore it.
[31] H. F. Cheung, Y. Gefen, E. K. Riedel, and W. H. Shih, Phys. Rev. B **37**, 6050 (1988). There is an error in the legend of Fig. 3. The letter (a) actually labelizes the even number and (b) the odd.
[32] P. W. Anderson, Phys. Rev. **109**, 1492 (1958).
[33] Y. Imry, *Introduction to Mesoscopic Physics* (Oxford University Press, New York, 1997).
[34] H. Cheung, E. K. Riedel, and Y. Gefen, Phys. Rev. Lett. **62**, 587 (1989).
[35] H. Bouchiat and G. Montambaux, J. Phys. (Paris) **50**, 2695 (1989); G. Montambaux, H. Bouchiat, and R. Friesner, Phys. Rev. B **42**, 7647 (1990).
[36] A. Altland, Y. Gefen, and G. Montambaux, Phys. Rev. Lett. **76**, 1130 (1996).
[37] J. C. Charlier, J. P. Michenaud, and P. Lambin, Phys. Rev. B **46**, 4540 (1992).
[38] P. Lambin, V. Meunier, and A. Rubio, Phys. Rev. B **62**, 5129 (2000).
[39] G. Dresselhaus *et al.*, in *Science and Application of Nanotubes*, edited by Tománek and R. J. Enbody (Kluwer, New York, 2000).
[40] L. Liu, C. S. Jahanthi, H. Guo, and S. Y. Wu, Phys. Rev. B **64**, 033414 (2000).
[41] A. Rochefort, D. R. Salahub, and P. Avouris, J. Phys. Chem. B **103**, 641 (1999).
[42] A. Rubio, D. Sanchez-Portal, E. Artacho, P. Ordejn, and J. M. Soler, Phys. Rev. Lett. **82**, 3520 (1999).
[43] D. Tomanek and S. G. Louie, Phys. Rev. B **37**, 8327 (1988).
[44] J.-C. Charlier, X. Gonze, and J.-P. Michenaud, Phys. Rev. B **43**, 4579 (1991); P. Lambin, L. Philippe, J. C. Charlier, and J. P. Michenaud, Comput. Mater. Sci. **2**, 350 (1994).
[45] L. Liu, G. Guo, C. Jayanthi, and S. Wu, Phys. Rev. Lett. **88**, 217206 (2002); S. Latil, S. Roche, A. Rubio, and P. Lambin (unpublished).